Reference: *Biol. Bull.* **183**: 220–232 (October, 1992)

Biological Consequences of Topography on Wave-swept Rocky Shores: I. Enhancement of External Fertilization

MARK DENNY, JEFF DAIRIKI[1], AND SANDRA DISTEFANO

Department of Biological Sciences, Stanford University, Hopkins Marine Station, Pacific Grove, California, 93950

Abstract. Surge channels on wave-swept rocky shores are characterized by the violent hydrodynamic mixing that accompanies broken waves. It has been suggested that this mixing rapidly dilutes gametes shed into the surf zone, thereby severely reducing the fraction of eggs that can be fertilized externally. Although surge channels are well mixed within themselves, field experiments show that the exchange of water between these small embayments and the adjacent mainstream is surprisingly slow. Thus, surge channels may act as "containment vessels," limiting the rate at which gametes are diluted, and thereby enhancing the efficacy of external fertilization. Indeed, a mathematical model of fertilization in surge channels suggests that given a sufficient population of adult males within a surge channel, 80–100% of eggs may be fertilized. This result must be tempered, however, by the possibility that the small-scale shears induced by turbulence interfere with fertilization.

Introduction

Recent field experiments with marine organisms have demonstrated that the fraction of eggs externally fertilized during spawning can be adversely affected by water motion. For example, when water velocity is 0.1–0.2 m s^{-1} and an individual male is separated from a female by more than 5 m, studies of sea urchins (Pennington, 1985; Levitan, 1991) and a hydroid (Yund, 1990) show that only 5–15% of eggs are fertilized. This low rate of fertilization is attributed to the dilution of gametes by turbulent mixing in flow. The percentage of eggs fertilized can be somewhat higher (approximately 30–50%) if multiple males are present, but is lower at higher velocities (Pennington, 1985; Levitan *et al.*, 1992). Even in fish that actively pair to spawn, the fraction of eggs fertilized can be low (40–50%) when the flow exceeds 0.1 m s^{-1} and wave-induced turbulence disperses the gametes (Petersen, 1991; Petersen, *et al.* 1992).

These studies (and the low rates of fertilization they report) raise important questions about the role of water motion in external fertilization and the consequences it may have in the evolution of reproductive strategies. However, flow during these experiments was relatively benign. How effective can external fertilization be under more extreme hydrodynamic conditions?

As ocean waves break upon rocky shores they generate water velocities as high as 15 m s^{-1} (Denny, 1988; Vogel, 1981), twenty to 100-fold faster than those in the studies cited above. These high velocities are accompanied by much more violent mixing of water. The "white water" characteristic of the surf zone is visual evidence of the extreme turbulence in breaking waves, and Denny and Shibata (1989) proposed that turbulence in the benthic boundary layer of the surf zone reduces the effectiveness of external fertilization well below even the low values measured subtidally. They estimate that only about 0.01–0.1% of eggs released into the surf zone are fertilized by a single adult male under typical conditions, and a maximum of only about 3% are fertilized when multiple males spawn synchronously. These predicted rates of fertilization are one to two orders of magnitude lower than those measured in subtidal flows, and suggest even more dramatic consequences for intertidal plants and animals than those proposed for subtidal organisms.

Denny and Shibata (1989) note, however, that the fraction of eggs fertilized in the surf zone could be sub-

Received 11 April 1992; accepted 27 July 1992.

[1] Present address: School of Oceanography WB-10, University of Washington, Seattle, Washington, 98195.

stantially higher than they predict if the volume into which gametes can be diluted is limited. Experiments described here show that blind-ended surge channels (the small-scale embayments typical of rocky shores) can act to limit the dilution volume for gametes of benthic organisms. Shoreline topography may thereby enhance the effectiveness of external fertilization in the surf zone, and the fraction of eggs fertilized in surge channels may actually be similar to that found in subtidal habitats.

Materials and Methods

Field experiments were conducted on the shoreline adjacent to Hopkins Marine Station, Pacific Grove, California. Four blind-ended surge channels (essentially, small-scale bays) were chosen to span the size typical of this coastline. Each was surveyed with a surveyor's level, tape measure, and stadial rod to provide the location (in cylindrical coordinates) of 100–150 points, and these points were analyzed (Surfer, Golden Software, Inc.) to produce a topographic map of each surge channel (Fig. 1). From these maps, the volume of each channel was estimated as a function of still water level (Fig. 2). Volume (at approximately the mean still-water level present during this study) ranged from 3.5 to 45 m^3.

The residence time of water in these channels was measured at high tide as follows. A control sample of water in the center of the channel was taken with a test tube attached to a wooden pole. For this and all subsequent samples, the tube was filled and emptied once before sampling to minimize the effects of any contaminants in the tube. Thirty grams of water-soluble fluorescein dye was dissolved in a liter of seawater, and 100–200 ml of the solution was introduced into the surge channel. The dye was allowed to mix throughout the channel until it appeared uniform, a process resulting from the entry of one to three breaking waves into the channel (10–30 s). Dipped samples were then taken at intervals of 15 or 30 s (depending on the rate of exchange between surge channel and mainstream) until the dye was no longer visible in the channel. Typically 15–30 samples were taken in each trial. Two trials were conducted for each channel on each sampling day. Trials were alternated between sites to allow dye to be thoroughly dispersed from each site prior to the second trial. Sample tubes were capped and kept in the dark until analyzed (usually the next day).

Markers were glued to one wall of each surge channel at 25 cm vertical intervals, allowing us to estimate visually (to within approximately 10 cm) the maximal and minimal height of the water's surface during each surge. Measurements were recorded in each channel, for each surge, during a 5 min period both before the first trial and after the last trial. The average of each 5-min series of readings provided an estimate of the mean, or still-water, level in the channel during the trial. The average of minimal heights provided an estimate of the mean low water level. The number of surges encountered, divided by the 5-min duration of the recording session, provided an estimate of the average period of the surge. Periods ranged from about 9–14 s. The height of each surge was estimated as the maximal height minus the subsequent minimal height. Heights recorded in each 5-min period were averaged to provide an estimate, H_{avg}, of the sea state during each trial. Average surge heights varied from 0.14 m to 0.74 m.

The concentration of dye in each sample was measured with an Aminco model SPF 500 spectrofluorometer and a standard series of dilutions from the stock dye solution. Concentrations were corrected for any background fluorescence present in the control sample, and were expressed as a fraction, C_r, of the concentration in the initial experimental sample. A model of the time series of relative concentrations from each trial was then determined by fitting the data to the equation:

$$C_r(t) = a \exp(-kt) + c; \qquad \text{(Eq. 1)}$$

a simplex algorithm (Caceci and Cacheris, 1984) was used to estimate the least-squares fit. The parameter c represents the quasi-equilibrium concentration of dye at the end of each trial when the concentration in the surge channel is equal to that in the adjacent mainstream flow. In all cases, c is small (typically <0.0001 a). The *exchange parameter* k represents the fraction of dye escaping from the surge channel in each interval of time t, and is thus a measure of the rate of exchange of water between surge channel and mainstream. The expected residence time, T_r, of a dye particle in the surge channel is

$$T_r = 1/k. \qquad \text{(Eq. 2)}$$

A total of 73 trials were conducted between October, 1988 and June, 1990. In three trials (4.1%), the measured concentrations in a surge channel appeared to increase substantially for one or more samples in the middle of the trial. These increases occurred too late in each trial to be attributed to incomplete initial mixing, and were due either to contamination in the sample tubes or to the accidental introduction of concentrated dye into the surge channel from an undetected "refuge" (a high tide pool, for example). Data from these anomalous trials were not included in the analysis.

A mixing model for blind-ended surge channels

As a means for examining our data, we formulated a simple model of the exchange between a surge channel and the mainstream. For the purposes of this model, the topography of a surge channel is represented by its volume versus still-water-level curve as shown in Figure 2. At the mean low water level determined for a trial, the channel holds a volume V_0. When a surge enters

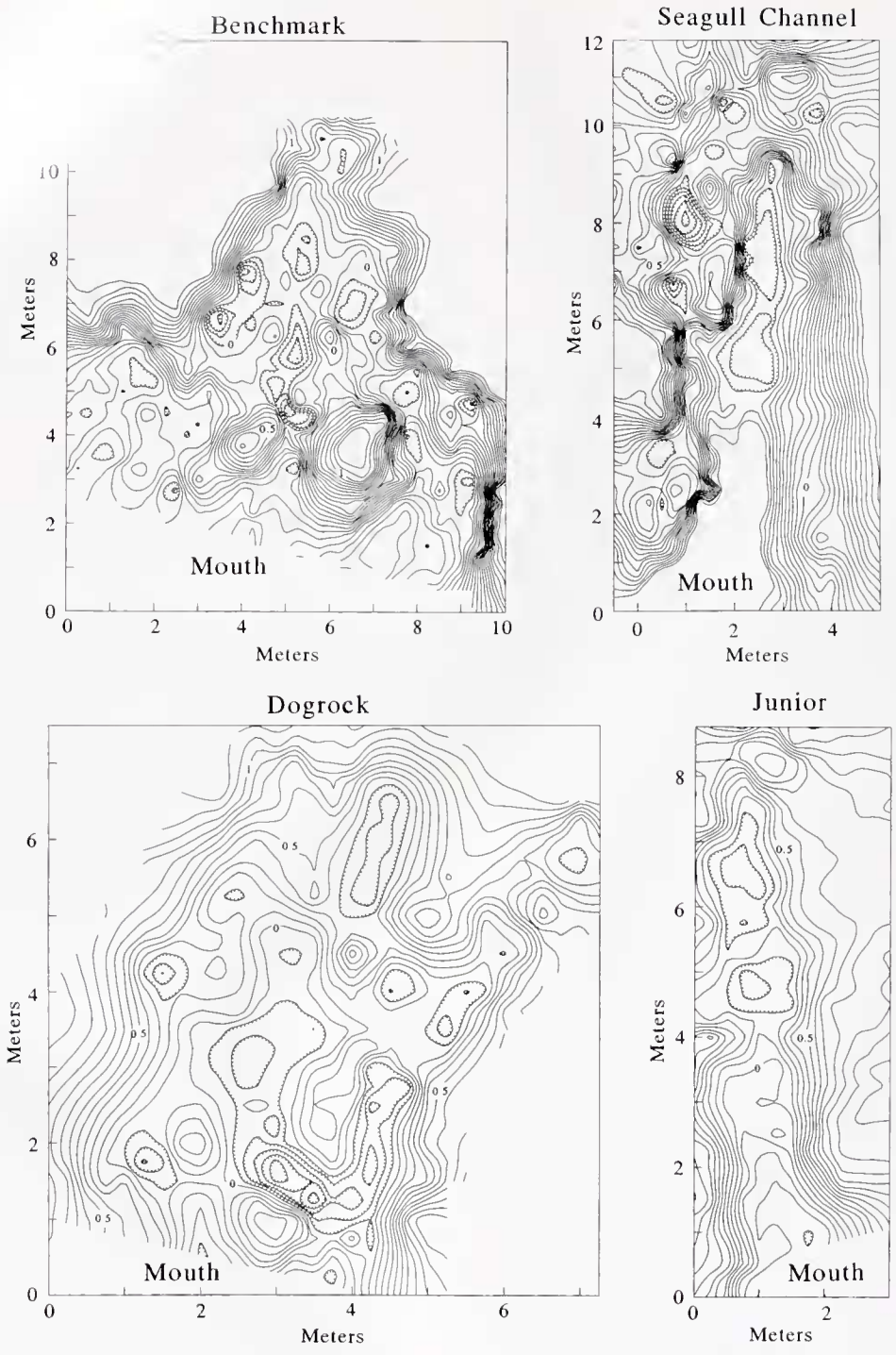

Figure 1. Topographical maps of the four embayments used in this study. Vertical gradations are 0.1 m; hachures denote local depressions.

the channel the water level rises, increasing the channel's volume by an amount ΔV. If the initial volume (V_0) and added volume (ΔV) are thoroughly mixed, the probability that a particle is carried out of the channel as the surge subsides and the water returns to its original level is

$$\text{Probability per surge} = \frac{\Delta V}{(V_0 + \Delta V)}. \quad \text{(Eq. 3)}$$

But the mixing of initial and added volumes may not be complete; in such a case the probability of escape from the channel is only a fraction, m, ($0 \leq m \leq 1$) of this

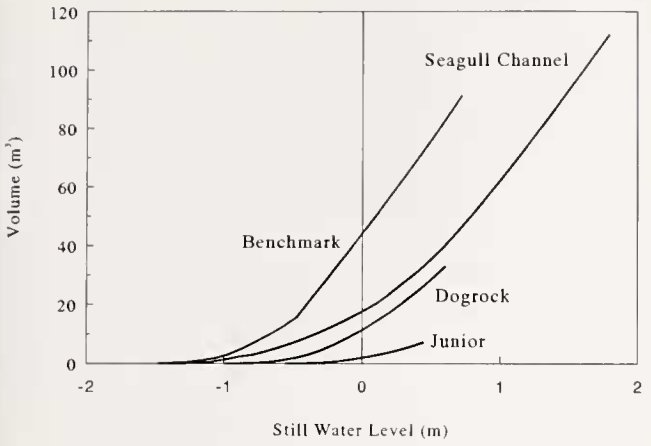

Figure 2. The relation between still water level and surge channel volume for the four embayments used in this study. These curves were calculated using the topographical maps of Figure 1.

maximal probability. If the average period between surges is T seconds, the probability that a dye particle is carried out of the channel in one second is thus

$$k = m \frac{\Delta V}{(V_0 + \Delta V)T}, \qquad \text{(Eq. 4)}$$

where k is again the exchange parameter of Eq. 1.

V_0, ΔV, T, and k can be determined experimentally, allowing us to calculate the *mixing parameter* m:

$$m \equiv \frac{k(V_0 + \Delta V)T}{\Delta V}. \qquad \text{(Eq. 5)}$$

Abundance of surge channels

The abundance of surge channels on a shore is strongly dependent on the local topography, and therefore may vary greatly from site to site. Due to the fractal nature of shorelines (Mandelbrot, 1982; Denny, in press), it is difficult to quantify precisely the abundance of surge channels for even a single site, because the exact location of the shoreline varies with the scale at which the shore is examined. An estimate of the abundance of surge channels on the shores at Hopkins Marine Station was made, however, using the following technique (Fig. 3).

An aerial photograph of the shore was traced onto paper to provide a two-dimensional representation of the shoreline with accurate detail present at a scale smaller than that used in the analysis. A point was chosen at random on this trace, and a caliper placed with one tip at this point. The caliper was then "walked" down the trace, and the distance between the tips of the caliper set the scale at which the shoreline was measured. The series of contiguous lines joining points where the caliper intersected the trace defined one realization of the "average" shoreline at that particular scale (Fig. 3). Segments of the actual shore that lie shoreward of this average were defined to be surge channels; segments seaward of the average shoreline were promontories. At each scale, the fraction of the average shoreline that comprised the mouths of surge channels, A, was then taken as a measure of relative surge channel abundance. This procedure was repeated for several starting points and the results averaged. The abundance of surge channels was measured at scales ranging from 2.2 to 22.4 m.

The shore at Hopkins Marine Station is formed from granite, and is not atypical of rocky shores on the west coast of North America.

Theory of external fertilization

If the exchange between water in surge channels and that in the adjacent mainstream is slow, then surge channels may function as "containment vessels" for gametes, thereby allowing for the effective fertilization of eggs. This possibility can be examined mathematically.

In this analysis, we follow the model of Denny and Shibata (1989), based primarily on data from sea urchins. Males are assumed to release sperm into a surge channel at a constant rate Q_s per second resulting in a concentration of sperm C_s (with units of m^{-3}) that may vary through time. Denny and Shibata (1989) also allowed C_s to vary in space, but for present purposes we assume that sperm are thoroughly mixed, ensuring that C_s is the same everywhere within the surge channel. Sperm (like dye particles) have a probability k in each second of passively escaping from the surge channel into the adjacent mainstream, and we assume that sperm that escape from the surge channel do not re-enter.

Sperm can swim and, under certain conditions, can move preferentially toward eggs (*e.g.*, Miller, 1985). The speed of sperm locomotion is very slow, however, a few tens of $\mu m\ s^{-1}$. In contrast, the motion of neutrally buoy-

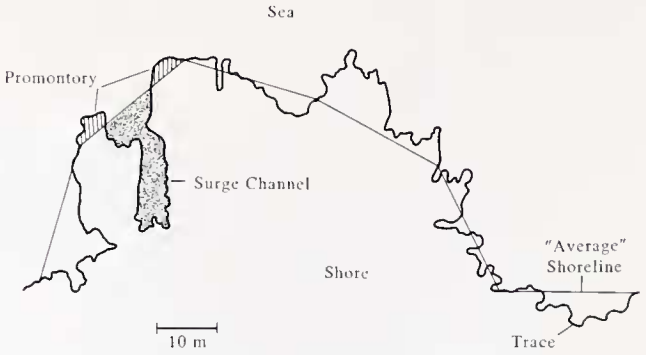

Figure 3. An example showing the traced shoreline (thick line), "average" shoreline at a particular scale (thin line segments), and the surge channel and promontory portions for a single segment of the average shore. This shoreline was traced from an aerial photograph of the shore at Hopkins Marine Station.

ant particles in turb[illegible]low can be characterized by a velocity u_* (the [illegible]ocity), a measure of the intensity of tur[illegible]low (Schlichting, 1979; Denny, 1988; Den[illegible]ata, 1989). For the intensely turbulent flo[illegible] the surf zone of wave-swept shores, u_* is app[illegible]ately equal to 0.1 u_{avg}, where u_{avg} is the ensemble average velocity of the water (see Denny, 1988; Denny and Shibata, 1989). Water velocities in the surf zone vary from approximately 1–15 m s^{-1} (Denny, 1988), suggesting that u_* is 0.1–1.5 m s^{-1}. Thus, the velocity imposed by turbulence is four to five orders of magnitude faster than a sperm's swimming speed, and we assume that the swimming speed of sperm can be safely neglected in the present context.

Given these assumptions, we see that the rate of change of sperm concentration is equal to the difference between the rate at which concentration increases due to the release of sperm and the rate at which concentration decreases due to the passive escape of sperm to the mainstream:

$$\frac{dC_s(t)}{dt} = \frac{Q_s}{V} - kC_s(t), \qquad \text{(Eq. 6)}$$

where V is the still-water volume of the surge channel.

If we assume that $C_s(0) = 0$, we calculate that

$$C_s(t) = \frac{Q_s}{kV}[1 - \exp(-kt)]. \qquad \text{(Eq. 7)}$$

At infinite time C_s reaches a steady-state concentration, $C_{s,\infty}$:

$$C_{s,\infty} = \frac{Q_s}{kV}. \qquad \text{(Eq. 8)}$$

We assume that females release eggs at the constant rate Q_e per second, and that eggs are mixed and exchanged as for sperm. Thus,

$$\frac{dC_e(t)}{dt} = \frac{Q_e}{V} - kC_e(t), \qquad \text{(Eq. 9)}$$

$$C_e(t) = \frac{Q_e}{kV}[1 - \exp(-kt)], \qquad \text{(Eq. 10)}$$

$$C_{e,\infty} = \frac{Q_e}{kV}, \qquad \text{(Eq. 11)}$$

where C_e is the instantaneous concentration of eggs (m^{-3}) and $C_{e,\infty}$ is the steady-state concentration.

We assume that the rate at which sperm fertilize eggs is governed by the co-occurring concentrations of both sperm and eggs and by a "reaction" parameter, ϕ.

$$\text{Rate of fertilization} = \phi C_{s,v}(t)C_{e,v}(t). \qquad \text{(Eq. 12)}$$

Here, $C_{s,v}$ and $C_{e,v}$ are the concentrations of unattached sperm and virgin eggs, respectively.

The reaction parameter is the product of the effective speed at which sperm are mixed through the water (here assumed to be the friction velocity u_*) and the effective "collision cross section" of an egg (Denny and Shibata, 1989), and has units $m^3\ s^{-1}$.

If an egg could be fertilized by the first sperm that contacted any point on its surface, the "collision cross section" would be the same as the projected area of the egg. For sea urchin eggs with a diameter of 10^{-4} m this is 7.85×10^{-9} m^2. Laboratory measurements suggest, however, that sea urchin eggs behave as if only a small fraction of their surface area is fertilizable. The reason for this reduced cross section is unclear. Vogel *et al.* (1982) suggest that apparent fertilizable area is only about 1% of the overall area for *Paracentrotus lividus*. More recent experiments with *Strongylocentrotus franciscanus* (Levitan *et al.*, 1991) suggest an apparent fraction of 3%. Using this latter value, we find that

$$\phi = u_*(2.4 \times 10^{-10}\ m^2), \qquad \text{(Eq. 13)}$$

and because $u_* \approx 0.1u_{avg}$,

$$\phi \approx u_{avg}(2.4 \times 10^{-11}\ m^2). \qquad \text{(Eq. 14)}$$

Given that average water velocities in the surf zone vary from approximately 1 to 15 m s^{-1}, ϕ is likely to vary from 2.4×10^{-11} to 3.5×10^{-10} $m^3\ s^{-1}$.

Denny and Shibata (1989) calculated that an individual urchin extrudes sperm at approximately $10^7\ s^{-1}$ or eggs at $10^4\ s^{-1}$, and these values are used here. Due to the vast overabundance of sperm it seems safe to assume that the concentration of sperm is minimally affected by the attachment of sperm to eggs; thus

$$C_{s,v} = C_s. \qquad \text{(Eq. 15)}$$

Given these assumptions, we can describe the flux of virgin eggs through a surge channel. Virgin eggs are added to the local population as they are released by females and are removed either by escaping to the mainstream or by fertilization. Thus:

$$\frac{dC_{e,v}(t)}{dt} = \frac{Q_e}{V} - kC_{e,v}(t) - \phi C_s(t)C_{e,v}(t). \qquad \text{(Eq. 16)}$$

At this point the mathematics can be simplified if we convert each of the variables of interest to a dimensionless form. In the present context, time is important primarily as it relates to the residence time of gametes in a surge channel. Thus we may specify a dimensionless time τ,

$$\tau = t/T_r = kt. \qquad \text{(Eq. 17)}$$

Note that

$$\frac{dg}{d\tau} = \frac{dg}{dt}\frac{dt}{d\tau} = \frac{1}{k}\frac{dg}{dt} \qquad \text{(Eq. 18)}$$

for any function g.

The instantaneous concentration of eggs can be expressed in dimensionless form by dividing by the steady-state concentration of eggs. Thus,

$$e(\tau) \equiv \frac{C_e(\tau)}{C_{e,\infty}} = \frac{C_e(\tau)}{(Q_e/kV)}. \qquad \text{(Eq. 19)}$$

Similarly, the instantaneous concentration of virgin eggs is:

$$v(\tau) \equiv \frac{C_{e,v}(\tau)}{C_{e,\infty}} = \frac{C_{e,v}(\tau)}{(Q_e/kV)}. \qquad \text{(Eq. 20)}$$

The instantaneous concentration of sperm is made dimensionless by expressing it as a fraction of the steady-state concentration of sperm:

$$s(\tau) \equiv \frac{C_s(\tau)}{C_{s,\infty}} = \frac{C_s(\tau)}{(Q_s/kV)}. \qquad \text{(Eq. 21)}$$

Finally, we devise a dimensionless fertilization parameter Θ that incorporates several of the variables that govern the rate of fertilization:

$$\Theta \equiv \frac{\phi}{k} C_{s,\infty} = \frac{\phi Q_s}{k^2 V} = \frac{\phi Q_s T_r^2}{V}. \qquad \text{(Eq. 22)}$$

Inserting these dimensionless variables into our previous results (Eqs. 7, 8, 10, 11, and 16), we find that:

$$s(\tau) = e(\tau) = 1 - \exp(-\tau), \qquad \text{(Eq. 23)}$$

$$s_\infty = e_\infty = 1, \qquad \text{(Eq. 24)}$$

$$\frac{dv(\tau)}{d\tau} = 1 - v(\tau) - \Theta s(\tau) v(\tau). \qquad \text{(Eq. 25)}$$

Thus, at steady state (that is, when $dv(\tau)/d\tau = 0$),

$$v_\infty = 1/(1 + \Theta). \qquad \text{(Eq. 26)}$$

In other words, the larger Θ is, the lower the steady-state fraction of virgin eggs, v_∞. A large Θ can result from a large rate of sperm release (for example, due to the presence of multiple males), a small surge channel volume, an intense level of turbulence, or a long residence time (Eq. 22). Thus, any combination of these factors produces a lowered fraction of virgin eggs. Note, however, that Θ scales with the square of residence time, so v_∞ is especially sensitive to T_r (or, equivalently, to k).

Now, the concentration of fertilized eggs is equal to the difference between the total concentration of eggs and the concentration of virgin eggs. By analogy, the *fraction* of all eggs that are fertilized, $f(\tau)$, is equal to $1 - v(\tau)$. From Equation 26 we see that at steady-state

$$f_\infty = \Theta/(1 + \Theta). \qquad \text{(Eq. 27)}$$

Non-steady-state conditions

This result applies to surge channels once they have reached a steady-state concentration of gametes. Is it realistic to apply these steady-state results to the real world? To answer this question, we solved Equation 25 for v as a function of τ using an implicit trapazoidal finite difference technique:

$$v([i+1]\delta\tau) = v(i\delta\tau)\frac{\{1 - (\delta\tau/2)[1 + \Theta - \Theta \exp - (i\delta\tau + \tfrac{1}{2}\delta\tau)]\}}{\{1 + (\delta\tau/2)[1 + \Theta - \Theta \exp - (i\delta\tau + \tfrac{1}{2}\delta\tau)]\}} + \frac{\delta\tau}{\{1 + (\delta\tau/2)[1 + \Theta - \Theta \exp - (i\delta\tau + \tfrac{1}{2}\delta\tau)]\}}, \qquad \text{(Eq. 28)}$$

where $\delta\tau$ is the time step and i is a counter (i = 0, 1, 2, 3, . . .). At $\tau = 0$, all eggs are assumed to be virgin so that $v(0) = 1$.

We again set $f = 1 - v$ and follow f as a function of dimensionless time.

Results

Mixing in surge channels

The decrease in dye concentration within a surge channel is modeled accurately by the exponential decrease of Equation 1 (Fig. 4). The average coefficient of determination (r^2) for the 70 trials is 0.955 (with a standard deviation of 0.054), indicating that, to a first approximation, each dye particle can be regarded as having a fixed probability of escaping from the surge channel in a given interval.

Exchange between surge channel and mainstream water is surprisingly slow. The exchange parameter k varies from approximately 0.001 to 0.04, implying average residence times, T_r, of 25 to 1000 s.

The mixing parameter, m, varies from about 0.05 to 0.9. When data from all four surge channels are combined, m is found to be an increasing function of average surge height (Fig. 5), but variation in H_{avg} explains only 17% of the variation in m. The mixing parameter is not significantly correlated with the average fractional change in volume during a downsurge, $\Delta V/(V_0 + \Delta V)$ ($r = 0.0619$, 68 df, $P > 0.5$).

When data from all four surge channels are combined, the exchange parameter k is found to be an increasing function of average surge height (Fig. 6), and the relationship explains 51% of the variation in k. The exchange parameter is also positively correlated with the fractional change in volume in the surge channel, which is itself a direct function of H_{avg}, but the correlation ($k = 0.179\ H_{avg} + 0.0023$, $r = 0.431$, 68 df) explains much less of the variation than does surge height alone (19 *vs.* 51%).

Abundance of surge channels

Surge channels form about 46% of the shoreline at Hopkins Marine Station (Table 1). The fractional abundance of surge channels is not correlated with the scale at which the shoreline is measured ($r = 0.134$, 3 df, $P > 0.5$), at least for the range of scales examined here.

Predicted fraction of eggs fertilized

At a realistic value of Θ (that is, a realistic combination of k, V, ϕ, and Q_s), a substantial fraction of eggs is expected

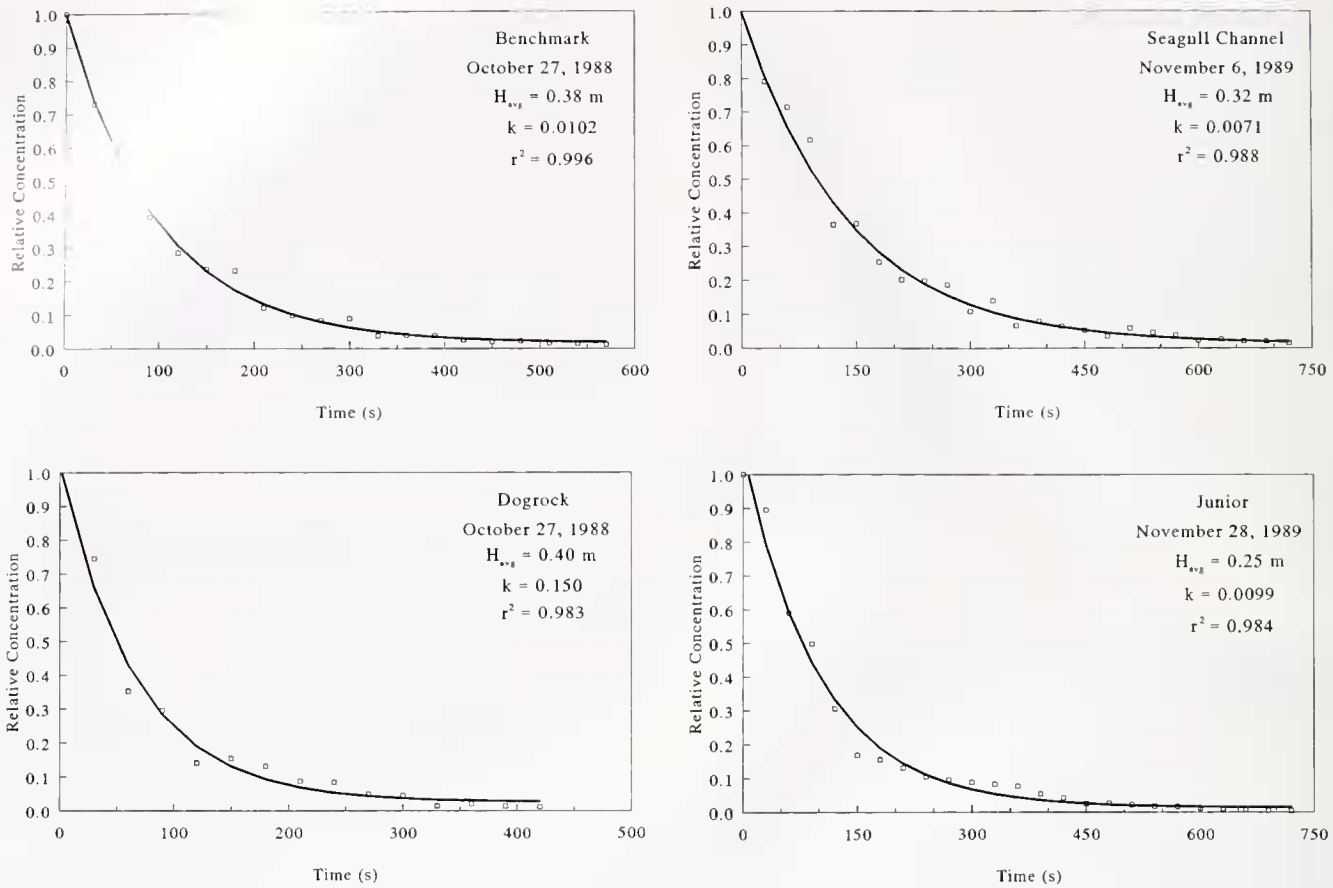

Figure 4. Representative examples of the temporal decay in dye concentration in the experimental embayments. The solid curves are least-squares fits to the data using the model of Equation 1.

to be fertilized (Fig. 7). For example, if ϕ is 10^{-10} m^3 s^{-1}, and the residence time is 50 s ($k = 0.02$ s^{-1}) for a surge channel with a volume of 10 m^3 (typical values for the shore at Hopkins Marine Station), about 20% of eggs can be fertilized by a single male. This is two to three orders of magnitude larger than the fraction predicted by Denny and Shibata (1989) for flow outside of surge channels.

Multiple males

Increasing the number of males present in a surge channel increases Q_s, with a concomitant increase in Θ, and thereby an increase in the fraction of eggs fertilized (Fig. 8). Consider, for instance, a surge channel with the same residence time as that cited above ($k = 0.02$ s^{-1}), but with five times the volume (50 m^3). If this channel has an average still water depth of 1 m, it has approximately 70 m^2 of substratum area. Even given the fivefold increase in volume, if only 3 males are present per square meter of substratum (210 males total, a realistic value for wave-swept shores), 90% of eggs are expected to be fertilized.

Smaller channels will have a larger ratio of substratum area to channel volume. Thus, given the same spatial density of male urchins, smaller channels will have a higher fraction of eggs fertilized.

Time dependence of fertilization

The time-dependent fraction of eggs fertilized is shown in Figure 9a. For realistic values of Θ, values of f within 10% of steady-state values are obtained within a period of 5 T_r. For a typical residence time of 50–120 s, this implies that the steady-state estimate of fertilization fraction is reached within 4–10 minutes. Given that an individual urchin in the laboratory releases gametes for approximately 1 h, equilibrium conditions are likely to apply to most gametes released.

Note that Figure 9a shows the fraction of eggs fertilized relative to the steady-state fraction. The absolute fraction fertilized is shown as a function of dimensionless time in Figure 9b. The fraction fertilized decreases with decreasing Θ as expected.

Discussion

Mixing in small surge channels

The rate of exchange between small, well-mixed surge channels and mainstream waters is both a simple and a

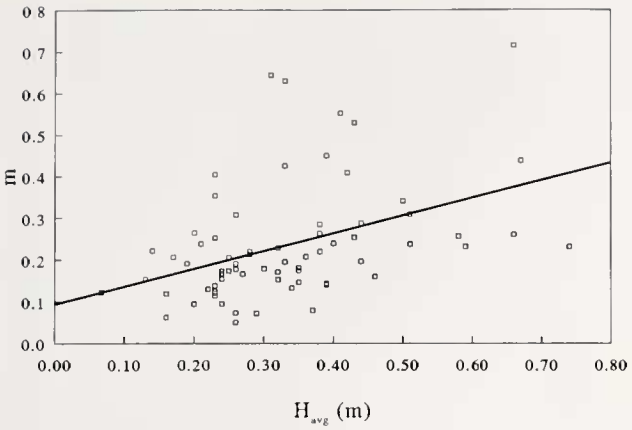

Figure 5. The relation between average surge height (H_{avg}) and the dimensionless mixing parameter, m. The linear regression (solid line) explains approximately 17% of the variation in m: $m = 0.424 \times H_{avg} + 0.094$ ($r^2 = 0.173$), where H_{avg} is measured in m.

complex process. Our data indicate that the probability per time that a small, inanimate, neutrally buoyant particle will escape from a surge channel is constant for at least a few tens of minutes, and that this probability can be predicted with reasonable accuracy from the height of the surge present in the surge channel. In this respect the results of the process are simple to predict as shown in Figure 6.

It is more difficult to account for these predictions on a mechanistic basis, primarily because of the variability of the mixing parameter, m. At present, m cannot be predicted accurately, from either average surge height (Fig. 4) or fractional change in volume. Probably, m is affected by the local topography of each surge channel and by chance variation in the shape of each breaking wave, rendering it of little value as a general predictive tool.

Note that the relationship measured here between surge height and exchange parameter (Fig. 6) can be applied

Table 1

Fraction of the average shoreline that comprises the mouths of surge channels at Hopkins Marine Station

Scale (m)	Fraction, A
2.2	0.446
4.5	0.440
9.0	0.508
22.4	0.455

only to a relatively narrow range of channel sizes. There is a lower limit to the size at which a local indentation in the shoreline can be considered a surge channel for our purposes. If the still-water depth in the indentation is less than the amplitude of the surge ($=H_{avg}/2$), the indentation is completely emptied by an average downsurge, and the probability of a particle re-entering the channel on the subsequent upsurge is set more by mainstream mixing and advection than by mixing within the indentation itself. In this case, the indentation is not a surge channel in the sense that we have used the term here.

The upper limit to the size of this relationship is set by the size at which a surge channel is no longer well mixed within itself. Only if the channel is well mixed can Equation 1 accurately model residence time. We have noticed distinct advective patterns in bays in excess of the size studied here—particles that enter a larger bay at one portion of its mouth predictably exit at another specific region. In this case, the probability of exchange for a particle depends in part on its history, and the simple model of Equation 1 cannot be expected to hold. Thus, the predictions implicit in Figure 6 should not be applied to surge channels larger than approximately 100 m^3.

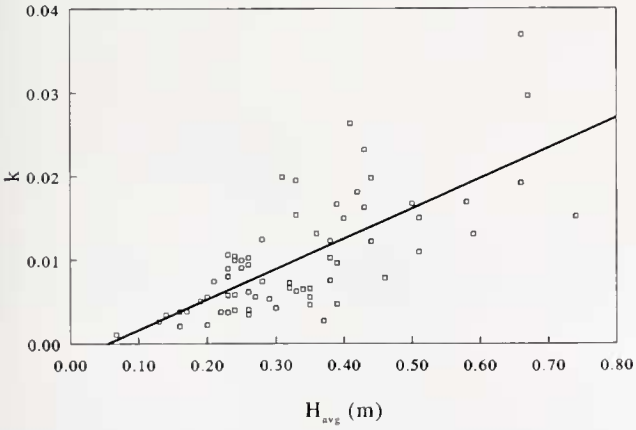

Figure 6. The relation between average surge height (H_{avg}) and the exchange parameter k. The linear regression (solid line) explains approximately 51% of the variation in k: $k = 0.036 \times H_{avg} + 0.002$ ($r^2 = 0.514$), where H_{avg} is measured in m, and k has the units s^{-1}.

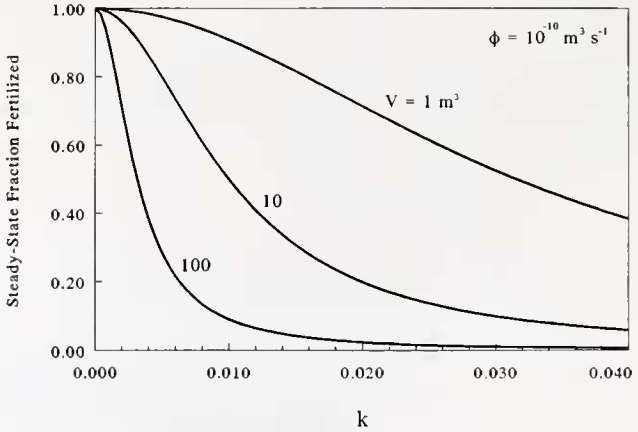

Figure 7. As the probability of gametes escaping from a surge channel increases, the equilibrium fraction of eggs fertilized decreases. The larger the volume of the surge channel (V), the lower the fraction of eggs fertilized.

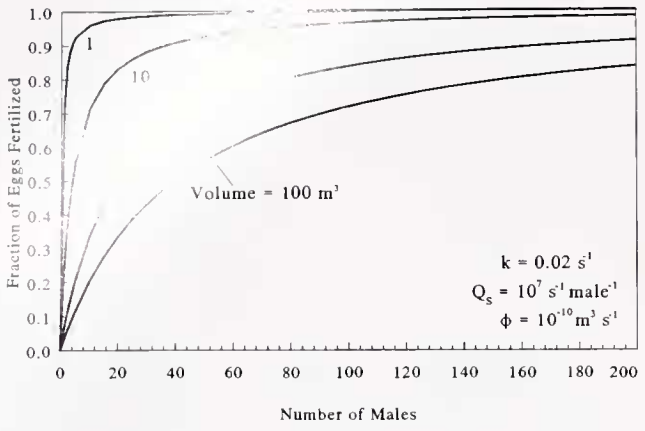

Figure 8. The fraction of eggs fertilized increases with the number of males present in a surge channel.

The fraction of eggs fertilized

The predictions made here suggest that external fertilization in surge channels may be quite effective, with fertilization fractions comparable to or exceeding those measured for benthic invertebrates in relatively benign subtidal flows (Pennington, 1985; Yund, 1990; Levitan, 1991; Levitan *et al.*, 1992). If these predictions are valid, fertilization may be much less of a limiting process than suggested by the model of Denny and Shibata (1989), at least within surge channels.

Furthermore, about 46% of the shoreline at Hopkins Marine Station is formed of surge channels (Table II). If we assume that the fraction of eggs fertilized within the surf zone, but outside of surge channels, is equal to the maximal fraction predicted by Denny and Shibata (1989) (3%), and that individuals are randomly distributed along the shore, then the overall fraction of eggs fertilized is approximately

$$\text{Overall fraction} = (f - 0.03)A + 0.03, \quad \text{(Eq. 29)}$$

where f is again the steady-state fraction of eggs fertilized in surge channels, and A is the fraction of shoreline that comprises the mouths of channels. For f = 0.9 and A = 0.46, the overall fraction of eggs fertilized is thus 43%, suggesting that external fertilization in the surf zone, taken as a whole, may be considerably higher than that suggested by Denny and Shibata (1989).

The role of shoreline topography in controlling the overall rate of external fertilization is clear in Equation 29. If the shore is constructed of rocks that are not susceptible to the formation of surge channels, A will be small, and the overall fraction of eggs fertilized will be similarly small. Conversely, on a shore where surge channels are abundant, external fertilization may be quite effective.

Localized fertilization

Denny and Shibata (1989) concluded that, as long as there is no practical limit to the volume into which eggs and sperm are mixed, dilution of gametes is so rapid that those few eggs that are fertilized are likely to be fertilized by sperm from the nearest males. In this fashion, rapid dilution insures the localization of fertilization.

As a corollary to the effectiveness of fertilization in surge channels, we note the implication that the long residence time of water in channels can again lead to localization of fertilization. Once gametes escape from a channel they are subject to the infinite dilution described by Denny and Shibata (1989), and subsequent fertilization becomes highly unlikely. Eggs released in a surge channel are therefore very likely to be fertilized by males in the same channel. Thus both infinite dilution and the limitation of dilution result in localized fertilization, leading us to suppose that, as a general rule, external fertilization in the surf zone can be effective only over short distances.

The effect of localized fertilization due to surge channels on the population genetics of a species is unclear. Although the residence time of small surge channels is surprisingly long, it is still short compared to the larval lifetime of most species, which vary from a few hours to several

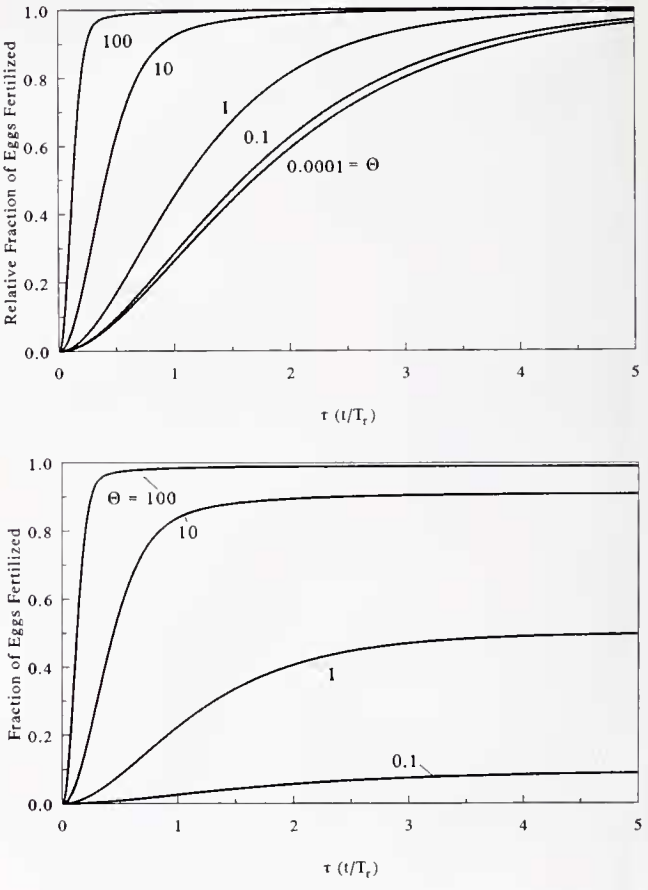

Figure 9. (A) Steady-state conditions are approached within a period equal to 5 times the retention time ($\tau = 5$). The fraction of eggs fertilized is expressed as a fraction of the steady-state value. (B) The actual fraction of eggs fertilized is plotted without being normalized to the fraction at steady state.

months. As a result, although fertilization may be localized, the resulting larvae are free to participate in the larger-scale dynamics of the population. We recognize that the long residence time of surge channels may have important implications for the spatial pattern of settlement of larvae, as well as for the probability that newly fertilized embryos will be consumed by benthic suspension feeders, but these implications will not be developed here.

Instantaneous mixing, shear stress, and a note of caution

We foresee two factors that could affect the results presented here.

First, the model of external fertilization assumes that gametes are instantaneously mixed throughout a surge channel. As noted, however, thorough mixing within a channel requires the entry of one to three breaking waves. In the brief period prior to the arrival of the first wave, local high concentrations of gametes may be present, and if eggs encounter an area of high sperm concentration, the probability of fertilization may be very high. Note, however, that any momentary reduction in mixing that allows a high concentration of sperm to be maintained also reduces the probability that an egg will be delivered, by chance, to that area of high concentration. Quantitative analysis of the dynamics of fertilization over times shorter than the period of the surge will require a more complete understanding of the structure of turbulence within surge channels than is currently available.

Second, the calculations made here are based on the assumption that sperm and eggs interact in a fashion akin to molecules in a gas. If a sperm happens to be in the vicinity of an egg and aimed in the right direction, it impacts on the egg, sticks, and (perhaps) fertilization follows. However, this simple view ignores the small-scale hydrodynamics relevant to sperm and eggs, and as a result may overestimate the probability of fertilization.

To see why, we explore flow in the surf zone at the spatial scale of a gamete. This exploration is carried out in two steps. First, we examine the rate at which turbulent kinetic energy is dissipated in the surf zone. Next, we use these results to estimate the average velocity gradient to which gametes are subjected. The biological consequences of this gradient can then be discussed.

Ocean waves carry energy with them as they approach the shore. The rate, P, at which wave energy is transported across the mouth of a surge channel M meters wide is

$$P \approx (1/8)\rho g H^2 M (2gH)^{1/2}$$
$$\approx 0.177 \rho g^{3/2} H^{5/2} M, \qquad \text{(Eq. 30)}$$

where ρ is the density of seawater (approximately 1025 kg m^{-3}), g is the acceleration due to gravity (9.81 m s^{-1}), and H is wave height (Denny, 1988). Thus, the power per meter of surge channel mouth, P′, is

$$P' \approx 0.177 \rho g^{3/2} H^{5/2}. \qquad \text{(Eq. 31)}$$

In making this calculation we have assumed that wave height at breaking is equal to water depth (Denny, 1988), and that waves at breaking move at the speed predicted by solitary wave theory (in this case, $(2gH)^{1/2}$ [Denny, 1988]).

Some of this incident wave energy may be carried back out of the surge channel if the wave reflects from the shore. If the height of the reflected wave is a fraction R of the incoming wave height ($0 \le R < 1$), the net power delivered to the channel (per meter of channel mouth) is

$$P'_n \approx 0.177 \rho g^{3/2} H^{5/2} (1 - R^{5/2}). \qquad \text{(Eq. 32)}$$

On rocky shores, R (the *reflection coefficient*) is typically small. For example, the R for a rubble breakwater (similar in topography to a rocky shore) is less than 0.29 when the slope of the breakwater is 1:5 (U.S. Army Corps of Engineers, 1984). If the slope is 1:10, the reflection coefficient is less than 0.13. If energy is transported inshore by waves but only a small fraction is carried back out by waves, most of the incident wave power must either be dissipated in the surf zone or transported out by other means (*e.g.*, kinetic energy associated with an undertow, acoustic energy). Effective transport by these other mechanisms appears unlikely, and we assume here that most wave energy is dissipated in the surf zone.

The magnitude of this rate of energy dissipation can be estimated from a simple example. The bottom of a surge channel has a slope α, as shown in Figure 10, and the wave height at the mouth of the channel is equal to the depth at the mouth of the channel. Given these conditions, waves break near the channel mouth, and the entire net energy of the waves is dissipated within the channel.

The still-water volume of the surge channel per width of mouth is

$$V'_{swl} \approx \frac{H^2}{2 \tan \alpha}. \qquad \text{(Eq. 33)}$$

As a breaking wave moves into the channel, its height decreases as wave energy is first converted to tubulent kinetic energy and then dissipated. Thornton and Guza (1983) have shown that the average (root mean square)

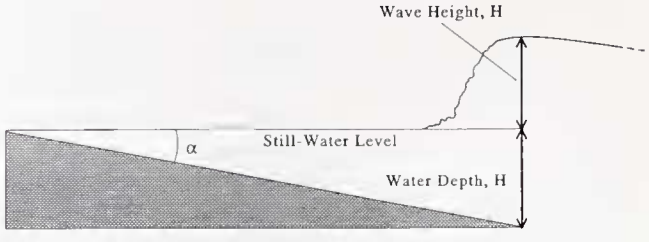

Figure 10. A schematic cross section through a surge channel illustrating the relation between bottom slope (α) and water depth, and showing the typical shape of a broken wave.

height of waves after [illegible] reak on a given shore is a constant fraction [illegible] al water depth. For a sandy beach, this fra[illegible] .4 and it is likely to be similar on rocky sh[illegible] e of computation, however, we use a val[illegible] s the broken wave propagates into the ch[illegible] ssume that its shape approximates that of a turb[illegible] ore; that is, it has a steep leading face, and the water level behind the face is nearly equal to that of the wave crest (Fig. 10). Given these assumptions, the broken wave increases the volume of water in the surge channel by maximally ¼ the channel's still-water value. Thus, the maximal effective volume of water in which the wave energy is dissipated is

$$V' \approx \frac{5H^2}{8 \tan \alpha} \qquad \text{(Eq. 34)}$$

The minimal rate at which wave energy is dissipated per unit of effective water volume (W′) in the surge channel is thus,

$$W' = P_n'/V' \approx 0.283\rho g^{3/2} H^{1/2}(1 - R^{5/2}) \tan \alpha. \qquad \text{(Eq. 35)}$$

Now, the turbulent kinetic energy due to wave breaking is ultimately dissipated as heat via the action of viscosity. This mechanism is elegantly described by Lazier and Mann (1989): at small spatial scales, turbulent eddies in the broken wave are damped by the water's viscosity, forming in their stead a linear velocity gradient (or shear) within the fluid that varies randomly in direction and strength. It is the interaction of this shear with viscosity that converts turbulent kinetic energy to heat.

The scale at which the chaotic motion of turbulent eddies is effectively damped can be estimated from the Kolmogorov length scale, L_v:

$$L_v = \left(\frac{\mu^3}{\rho^3 \epsilon}\right)^{1/4}, \qquad \text{(Eq. 36)}$$

where μ is the dynamic viscosity of seawater (1 to 2×10^{-3} Pa s, depending on temperature), ρ is again the water's density, and ϵ is the rate at which turbulent kinetic energy is dissipated per mass of fluid (W kg^{-1}). The largest shears are found in eddies with a diameter equal to approximately 40 L_v. Smaller eddies are much less energetic, and few eddies have a diameter less than 5–10 L_v (Lazier and Mann, 1989).

The fact that wave energy is dissipated via small-scale velocity gradients provides a method for examining the characteristics of flow on the spatial scale of eggs and sperm. Consider a small cubic volume of water with its top face moving relative to its bottom face such that a linear velocity gradient β (with units of s^{-1}) is established within the cube. As a result, the water in the cube is sheared. From Newton's law of viscosity (Vogel, 1981), we know that the shear stress (force per area) required to deform water at this rate is

$$\sigma = \mu\beta. \qquad \text{(Eq. 37)}$$

If the cube has sides of length dx, the force required to shear the cube is thus

$$F = dx^2 \mu\beta. \qquad \text{(Eq. 38)}$$

The power, P, dissipated by this force is equal to the product of force and velocity. The velocity at the top of the cube differs from that at the bottom by $dx\beta$. Therefore,

$$P = dx^3 \mu\beta^2. \qquad \text{(Eq. 39)}$$

The power dissipated per volume (dx^3) is thus

$$W' = \mu\beta^2, \qquad \text{(Eq. 40)}$$

and the power dissipated per mass is

$$\epsilon = \mu\beta^2/\rho. \qquad \text{(Eq. 41)}$$

Equating Equations 35 and 40 and solving for β, we find that the average velocity gradient in the fluid in a surge channel is:

$$\beta_{avg} \approx 0.532\rho^{1/2} g^{3/4} H^{1/4}(1 - R^{5/2})^{1/2}(\tan \alpha)^{1/2} \mu^{-1/2}, \qquad \text{(Eq. 42)}$$

and (from Eq. 37) the average shear stress in the fluid is

$$\sigma_{avg} \approx 0.532\rho^{1/2} g^{3/4} H^{1/4}(1 - R^{5/2})^{1/2}(\tan \alpha)^{1/2} \mu^{1/2}. \qquad \text{(Eq. 43)}$$

Note that these are *average* values for shear and shear stress. At any point in the fluid, instantaneous values likely vary through time. For each interval where the shear stress is lower than average, however, there must be a compensating interval in which stress is larger than average.

We are now in a position to evaluate directly the small-scale flow regime in surge channels and to explore its biological consequences.

For a slope of 1:5, a breaking wave height of 1 m, a reflection coefficient of 0.29, and a dynamic viscosity of 1×10^{-3} Pa s, the average rate of energy dissipation within a surge channel is 1.66 W kg^{-1} (Eqs. 40 and 41). From this value we estimate that the eddies associated with maximal shear stresses are approximately 1094 μm in diameter, 11–14 times the diameter of sea urchin eggs (80–100 μm). The smallest eddies likely to be found in surf-zone flow are about 137–273 μm in diameter. Even these small eddies are larger than typical gametes, suggesting that gametes in the surf zone experience a flow regime characterized primarily by linear shears rather than by turbulent eddies.

Note that the heat capacity of water is about 4200 J kg^{-1} K^{-1} (Weast, 1977). At the dissipation rate in this example, water is heated by only 0.0004°C s^{-1}. Thus, the energy dissipation within a surge channel is not sufficient to raise the temperature substantially, even for retention times of 100–1000 s.

For the typical conditions cited above, the average shear stress in the water is about 1.30 Pa, and the average mi-

croscale velocity gradient is 1304 s^{-1}. The presence of this gradient means that the velocity at one side of an egg is quite different from that at the opposite side, which causes the egg to rotate. The rate of rotation (in cycles per second) is (Happel and Brenner, 1983; Kessler, 1986)

$$\frac{\beta}{4\pi}. \qquad \text{(Eq. 44)}$$

In other words, an egg in a typical surf zone rotates on average about 104 times per second! Sperm oriented parallel to the velocity gradient (*i.e.*, the velocity at the tip of their flagellum is maximally different from that at their head) will also be rotated by the shear, but because sperm are elongated rather than spherical, rotation is likely to cease once the sperm lies perpendicular to the instantaneous gradient (*i.e.*, with its head and tail in flow at the same speed).

The practical results of the rapid rotation of eggs, the rapid re-orientation of sperm, and the large shear stresses in the fluid are difficult to estimate. Certainly the egg, as a solid object, will entrain fluid with it as it rotates, creating a complex, 3-dimensional, temporally variable boundary layer that must be crossed by sperm. Whether the rotation itself can affect contact between egg and sperm is less clear. Also unclear is whether surf-zone shear stresses are sufficient to dislodge sperm from the egg once they have attached, or to damage the sperm or egg directly, although Denny and Shibata (1989) note preliminary evidence that even low shear stresses can reduce the fraction of eggs fertilized in the laboratory.

While the precise effects of the small-scale flow regime are unclear, the motions of sperm and egg will surely be complex and highly dynamic in turbulent flow which may also impede effective contact and subsequent fertilization and development. As long as the effects of shear stress and egg rotation remain unknown, the calculations made here concerning the effectiveness of fertilization in surge channels must be taken with a grain of salt. If turbulence inhibits the contact and subsequent attachment of sperm to eggs, or if the rapid rotation of eggs is detrimental to their survival, the calculations made here may overestimate the effectiveness of fertilization.

Acknowledgments

We thank E. C. Bell, B. Gaylord, K. Mead, H. Lasker, C. Petersen, and an anonymous reviewer for helpful suggestions. This study was funded by NSF grant OCE-87-11688 to M. Denny.

Literature Cited

Caceci, M. S., and W. P. Cacheris. 1984. Fitting curves to data. *Byte* **9:** 340–362.

Denny, M. W. 1988. *Biology and the Mechanics of the Wave-Swept Environment.* Princeton University Press, Princeton, NJ. 329 pp.

Denny, M. W. in press. Roles of hydrodynamics in the study of life on wave-swept shores, in *Ecomorphology,* P. C. Wainwright and S. Reilly, eds. University of Chicago Press, Chicago, IL.

Denny, M. W., and M. F. Shibata. 1989. Consequences of surf-zone turbulence for settlement and external fertilization. *Am. Nat.* **134:** 859–889.

Happel, J., and H. Brenner. 1983. *Low Reynolds Number Hydrodynamics.* Martinus Nijhoff Publishers, Dordrecht. 553 pp.

Kessler, J. O. 1986. The external dynamics of swimming micro-organisms. Pp. 257–307 in *Progress in Phycological Research,* Vol. 4, F. E. Round and D. J. Chapman, eds. Biopress Ltd., Bristol.

Lazier, J. R. N., and K. H. Mann. 1989. Turbulence and diffusive layers around small organisms. *Deep-Sea Res.* **36:** 1721–1733.

Levitan, D. R. 1991. Influence of body size and population density on fertilization success and reproductive output in a free-spawning invertebrate. *Biol. Bull.* **181:** 261–268.

Levitan, D. R., M. A. Sewell, and F.-S. Chia. 1991. Kinetics of fertilization in the sea urchin *Strongylocentrotus franciscanus:* interaction of gamete dilution, age, and contact time. *Biol. Bull.* **181:** 371–378.

Levitan, D. R., M. A. Sewell, and F.-S. Chia. 1992. How distribution and abundance influence success in the sea urchin *Strongylocentrotus franciscanus. Ecology* **73:** 248–254.

Mandelbrot, B. B. 1982. *The Fractal Geometry of Nature.* W. H. Freeman and Co, New York. 460 pp.

Miller, R. 1985. Sperm chemo-orientation in the metazoa. Pp. 275–337 in *The Biology of Fertilization,* Vol. 2, C. B. Metz and A. Monroy, eds. Academic Press, New York.

Pennington, J. T. 1985. The ecology of fertilization of echinoid eggs: the consequences of sperm dilution, adult aggregation, and synchronous spawning. *Biol. Bull.* **169:** 417–430.

Petersen, C. W. 1991. Variation in fertilization rate in the tropical reef fish, *Halichores bivattus:* correlates and implications. *Biol. Bull.* **181:** 232–237.

Petersen, C. W., R. R. Warner, S. Cohen, H. C. Hess, and A. T. Sewell. 1992. Variable pelagic fertilization success: implications for mate choice and spatial patterns of mating. *Ecology* **73:** 391–401.

Schlichting, H. 1979. *Boundary Layer Theory.* 7th ed. McGraw Hill, New York. 817 pp.

Thornton, E. B., and R. T. Guza. 1983. Transformation of wave height distributions. *J. Geophys. Res.* **88:** 5925–5938.

U. S. Army Corps of Engineers. 1984. *Shore Protection Manual.* U. S. Government Printing Office, Washington, DC.

Vogel, H., G. Czihak, P. Chang, and W. Wolf. 1982. Fertilization kinetics of sea urchin eggs. *Math. Biosci.* **58:** 189–216.

Vogel, S. 1981. *Life in Moving Fluids.* Willard Grant Press, Boston, Massachusetts. 352 pp.

Weast, R. C. 1977. *Handbook of Chemistry and Physics.* Chemical Rubber Company, Cleveland, Ohio.

Yund, P. O. 1990. An *in situ* measurement of sperm dispersal in a colonial marine hydroid. *J Exp. Zool.* **253:** 102–106.

Appendix I

Symbols used in the text and the equation where each is defined or first used

Symbol	Definition	Units	Equation
A	Relative abundance of channels		29
$C_e(t)$	Concentration of eggs at time t	m^{-3}	9
$C_{e,v}(t)$	Concentration of virgin eggs	m^{-3}	16
$C_{e,\infty}$	Steady-state egg concentration	m^{-3}	11
$C_r(t)$	Relative dye concentration		1
$C_s(t)$	Concentration of sperm at time t	m^{-3}	6
$C_{s,v}$	Concentration of unattached sperm	m^{-3}	15
$C_{s,\infty}$	Steady-state sperm concentration	m^{-3}	8
$e(\tau)$	Dimensionless egg concentration		19
e_∞	Steady-state e		24
$f(\tau)$	Fraction of eggs fertilized		
f_∞	Steady-state fraction of fertilized eggs		27
F	Force	N	38
g	Acceleration due to gravity	$m\ s^{-2}$	30
H	Surge height	m	31
k	Exchange parameter	s^{-1}	1
L_v	Kolmogorov length scale	m	35
m	Mixing parameter		4
P	Energy flux into a surge channel	W	30
P′	Energy flux per meter of channel mouth	$W\ m^{-1}$	31
P'_n	Net P′	$W\ m^{-1}$	32
Q_e	Rate of egg release	s^{-1}	9
Q_s	Rate of sperm release	s^{-1}	6
R	Reflection coefficient		32
$s(\tau)$	Dimensionless sperm concentration		21
s_∞	Equilibrium s		24
t	Time	s	1
T	Period of the surge	s	4
T_r	Expected residence time (1/k)	s	2
u_{avg}	Mean water velocity	$m\ s^{-1}$	14
u_*	Friction velocity	$m\ s^{-1}$	13
$v(\tau)$	Dimensionless concentration of virgin eggs		20
v_∞	Equilibrium v		26
V	Channel volume at still water level	m^3	3
V_0	Surge channel volume at mean low water	m^3	3
V′	Maximal volume per meter of channel mouth	m^2	34
V'_{swl}	Volume per meter channel mouth at SWL	m^2	33
Δ V	Surge-induced increase in channel volume	m^3	3
W′	P'_n/V'	$W\ m^{-3}$	35
α	Bottom slope		33
β	Velocity gradient	s^{-1}	37
β_{avg}	Average velocity gradient	s^{-1}	42
ϵ	Rate of energy dissipation	$W\ kg^{-1}$	36
Θ	Dimensionless interaction parameter		22
μ	Dynamic viscosity of water	Pas	36
ρ	Water density	$kg\ m^{-3}$	30
σ	Shear stress	Pa	37
σ_{avg}	Average shear stress	Pa	43
τ	Dimensionless time		17
ϕ	Reaction parameter	$m^3\ s^{-1}$	12